Published in final edited form as:
Biosci Rep. 2012 February 1; 32(1): 71–81. doi:10.1042/BSR20110077.

Binding affinities of vascular endothelial growth factor (VEGF) for heparin-derived oligosaccharides

Wenjing Zhao[*], **Scott A. McCallum**[*], **Zhongping Xiao**[†], **Fuming Zhang**[‡], and **Robert J. Linhardt**[*,†,‡,§]

[*]Department of Biology, Center for Biotechnology and Interdisciplinary Studies, Rensselaer Polytechnic Institute, Troy, NY, 12180, USA

[†]Department of Chemistry and Chemical Biology, Center for Biotechnology and Interdisciplinary Studies, Rensselaer Polytechnic Institute, Troy, NY, 12180, USA

[‡]Department of Chemical and Biological Engineering, Center for Biotechnology and Interdisciplinary Studies, Rensselaer Polytechnic Institute, Troy, NY, 12180, USA

[§]Department of Biomedical Engineering, Center for Biotechnology and Interdisciplinary Studies, Rensselaer Polytechnic Institute, Troy, NY, 12180, USA

Abstract

Heparin and heparan sulphate (HS) exert their wide range of biological activities by interacting with extracellular protein ligands. Among these important protein ligands are various angiogenic growth factors and cytokines. HS-binding to vascular endothelial growth factor (VEGF) regulates multiple aspects of vascular development and function through its specific interaction with HS. Many studies have focused on HS-derived or HS-mimicking structures for the characterization of $VEGF_{165}$ interaction with HS. Using a heparinase 1-prepared small library of heparin-derived oligosaccharides ranging from hexasaccharide to octadecasaccharide, we systematically investigated the heparin-specific structural features required for VEGF binding. We report the apparent affinities for the association between the heparin-derived oligosaccharides with both $VEGF_{165}$ and $VEGF_{55}$, a peptide construct encompassing exclusively the heparin-binding domain of $VEGF_{165}$. An octasaccharide was the minimum size of oligosaccharide within the library to efficiently bind to both forms of VEGF and that a tetradecasaccharide displayed an effective binding affinity to $VEGF_{165}$ comparable to unfractionated heparin. The range of relative apparent binding affinities among VEGF and the panel of heparin-derived oligosaccharides demonstrate that VEGF binding affinity likely depends on the specific structural features of these oligosaccharides including their degree of sulphation and sugar ring stereochemistry and conformation. Notably, the unique 3-*O*-sulpho group found within the specific antithrombin binding site of heparin is not required for $VEGF_{165}$ binding. These findings afford new insight into the inherent kinetics and affinities for VEGF association with heparin and heparin-derived oligosaccharides with key residue specific modifications and may potentially benefit the future design of oligosaccharide-based anti-angiogenesis drugs.

Corresponding author: Robert J. Linhardt, Biotech Center 4005, 110 8th Street, Troy, NY 12180-3590, USA, linhar@rpi.edu, Tel: 518-276-3404, Fax: 518-276-3405.

AUTHOR CONTRIBUTIONS

Wenjing Zhao, Scott McCallum, Fuming Zhang, and Robert Linhardt designed the study. Wenjing Zhao carried out the experiments and drafted the manuscript. Fuming Zhang did the SPR data analysis. Zhongping Xiao produced heparin-derived oligosaccharide library. Robert Linhardt directed the project and revised the manuscript prior to submission.

Keywords

heparin; heparin-derived oligosaccharide; heparin binding domain; surface plasmon resonance (SPR); solution affinity; vascular endothelial growth factor (VEGF)

INTRODUCTION

Heparin and heparan sulphate are structurally related members of the glycosaminoglycan (GAG) family consisting of repeating disaccharide subunits of 1→4 linked hexuronic acid, β-D-glucuronic acid (GlcA) or α-L-iduronic acid (IdoA) and glucosamine, α-D-*N*–acetylglucosamine (GlcNAc) or α-D-*N*-sulphoglucosamine (GlcNS) [1,2]. The hexuronic acid residues in these GAGs are frequently found to be modified with a 2-*O*-sulpho group. The glucosamine residue is commonly modified with a 6-*O*-sulpho group (GlcNS6S and GlcNAc6S) and in rare cases with a 3-*O*-sulpho group (GlcNS3S and GlcNS3S6S). Heparin is more highly sulphated than its undersulphated counterpart HS, with an average of 2–3 sulpho groups per disaccharide compared with 0–2 sulpho groups per disaccharide for HS [1,2]. Despite their differences, heparin and HS contain identical disaccharide sequences but in different ratios. Unique sequences, such as the pentasaccharide comprising the antithrombin III (ATIII) binding site, are found in both heparin and HS [1,2].

Heparin and HS are biosynthesised as proteoglycans (PGs) as one or more GAG chains are covalently attached to a core protein [3]. While heparin-PGs are stored in mast cell granules, HS-PGs are ubiquitously expressed on the cell surface of most cell types and in the extracellular matrix (ECM), where they exert a wide range of biological functions through interaction with a variety of protein ligands involved in diverse cellular processes [4–7]. These interactions are principally based on ionic or H-bonding forces between the sulpho and carboxyl groups in the saccharide backbone and basic amino acid residues in the heparin (or HS)-binding protein [8,9]. HS-induced cellular functions are believed to be highly dependent on the structure of the engaged polysaccharide [8–10].

Vascular endothelial growth factor (VEGF) is a heparin-binding angiogenic growth factor that regulates multiple aspects of vascular development and function including stimulation of vasculogenesis and angiogenesis by promoting endothelial cell proliferation and migration [11,12]. For more than two decades, research has shown that the VEGF family of growth factors and its receptors play pivotal roles in tumour angiogenesis by regulating tumour growth, invasion and metastasis [13,14]. As a result of alternative mRNA splicing, VEGF exists in a number of isoforms with each having different biological properties. The polypeptide of the predominant $VEGF_{165}$ isoform contains two structurally independent domains. Plasmin cleavage of $VEGF_{165}$ generates a homodimer consisting two disulphide bond-linked amino-terminal polypeptides (residue 1–110, $VEGF_{110}$) and two identical 55-residue C-terminal fragments (residue 111–165, $VEGF_{55}$) [15]. The 110 residue N-terminal ‘receptor binding’ domain contains the dimerization sites, the binding sites for the tyrosine kinase receptors FLT-1 and KDR (also referred to as VEGFR1 and VEGFR2, respectively). The carboxyl-terminal heparin-binding domain (HBD) contains the binding sites for heparin and the KDR co-receptor neuropilin[16]. VEGF isoforms have diverse HBD structure whereas the receptor-binding domain is invariant [15].

Emerging studies on inhibition of tumour angiogenesis via targeting of relevant angiogenic growth factors have shown promising primary results both *in vitro* and *in vivo* for therapies using heparin and HS-based oligosaccharides [17–19]. These compounds competitively bind to heparin-binding growth factors, preventing their interaction with cell surface HSPGs and cytokine receptors and hence inhibit angiogenesis [17]. Low molecular weight heparin

(LMWH), as an example, has been demonstrated to be potent inhibitors of fibroblast growth factor (FGF) 2 and VEGF-mediated human microvascular endothelial cell proliferation[20,21]. Recent evidence has implicated the significance of HS oligosaccharides on suppression of endothelial cell migration, tube formation, and signaling induced by $VEGF_{165}$ and FGF2 [22]. Nevertheless, how the complex structure of heparin and HS saccharide affect angiogenesis with regard to the distinct binding affinities towards their protein ligands and abilities to activate the respective signaling pathways still remains largely unexplored. Previous attempts have been made on elucidating the structural features within HS that contribute to its binding with $VEGF_{165}$ [22,23]. Here we report the VEGF binding affinities of a small library of heparinase 1-prepared heparin-derived oligosaccharides with sizes ranging from hexasaccharide to octadecasaccharide. Influences including oligosaccharide size and sulphation towards heparin-specific $VEGF_{165}$ and $VEGF_{55}$ binding are investigated using surface plasmon resonance (SPR).

MATERIALS AND METHODS

Materials

Recombinant human $VEGF_{165}$ was purchased from R&D System (Minneapolis, MN). $VEGF_{55}$, corresponding to residues 111–165 of $VEGF_{165}$, was produced by plasmin (Haematologic Technologies, Inc., Essex Junction, VT) cleavage of $VEGF_{165}$ as previously described [24,25]. Cloning, expression and purification of the recombinant heparinase 1 (EC 4.2.2.7) from *F. heparinum* in *Escherichia coli* were performed essentially as described before [26]. Heparin sodium salt was obtained from porcine intestinal mucosa (Celsus Laboratories, Cincinnati, OH). Streptavidin (SA) sensor chip and HBS-EP buffer (10 mM HEPES, pH 7.4, 150 mM NaCl, 3.0 mM EDTA and 0.005% (*v/v*) surfactant P20) were purchased from BIAcore (GE Healthcare, Uppsala, Sweden). Buffers were filtered (0.22 μm) and degassed before use. SPR measurements were performed on a BIAcore 3000 (BIAcore) operated using the version software.

Preparation of the oligosaccharide library from heparin

A series of homogeneous oligosaccharides with sizes ranging from disaccharide to hexadecasaccharide have been isolated and sequenced from fractionated heparin in our laboratory [27]. Briefly, heparin was digested by heparinase 1 (1.5 U/g) at 30°C until 30% completion. The reaction mixture was then fractionated by gel permeation chromatography on a Bio-Gel P-10 column (BioRad, Hercules, CA) to obtain uniform-sized oligosaccharides. Fractions were subsequently desalted on a Bio-Gel P-2 column and freeze-dried. For oligosaccharides with defined structures, the lyophilised uniform-sized oligosaccharides with the degree of polymerization (dp) from dp6 to dp16 were further purified and separated on a semi-preparative SAX-HPLC column (Shimadzu, Kyoto, Japan) equipped with a 5 μm Spherisorb column of dimension 2.0 × 25 cm^2 (Waters, Milford, MA). Chromatographically purified peaks were analyzed by LC-MS (Agilent 1100 LC/MSD, Agilent Technologies, Inc. Wilmington, DE) under conditions previously described[27,28]. The structure of each purified oligosaccharide was determined by 1D and 2D NMR measured at 298 K on a Bruker Avance 600 II MHz (14.1 T) NMR spectrometer equipped with cryprobe with z-axis gradients [27,29].

Immobilisation of biotinylated heparin onto streptavidin sensor chip

Biotinylated heparin was prepared by homogeneously reacting sulpho-*N*-hydroxysuccinimide long-chain biotin (Piece, Rockford, IL) with free amino groups of unsubstituted glucosamine residues in the polysaccharide chain (2.8 wt% of D-GlcN) according to a published procedure [30,31]. The biotinylated heparin was immobilised to streptavidin chip based on the manufacturer's protocol. Briefly, 20-μL solution of the

heparin-biotin conjugate (0.1 mg/mL) in HBS-EP running buffer was injected over flow cell 2 (FC2) of the SA chip at a flow rate of 10 μL/min. The successful immobilization of heparin was confirmed by the observation of a ~100 resonance unit (RU) increase in the sensor chip. The control flow cell (FC1) was prepared by 1 min injection with saturated biotin.

SPR-based kinetics measurement of the interaction between VEGF and heparin

A series of VEGF protein samples were prepared by dilution in HBS-EP buffer to final concentrations ranging from 0.63 nM to 10 nM and 10 nM to 150 nM for $VEGF_{165}$ and $VEGF_{55}$, respectively. Protein samples were injected at a flow rate of 30 μL/min. At the end of sample injection (180 s), HBS-EP buffer was passed over the sensor surface for 180 s during which VEGF dissociation was monitored. After dissociation, the sensor surface was regenerated by injecting 2 M NaCl to remove all the binding proteins. The response was monitored as a function of time (sensorgram) at 25 °C. Apparent rate constants for chip association were obtained in global fits to the SPR data at multiple protein concentrations with residuals for the resulting fits being used to assess the goodness of the fit. BIAevaluation 3.0 software was used for all SPR data analysis.

Inhibition of VEGF binding to heparin-coated chip by heparin-derived oligosaccharides in solution

A $VEGF_{165}$ (5 nM) or $VEGF_{55}$ (100 nM) sample was premixed with 1 μM of each uniform-sized heparin oligosaccharide mixture (dp6–dp18) or each structurally defined oligosaccharide (dp8–dp16) in HBS-EP buffer. The mixed solution was injected over the heparin chip at a flow rate of 30 μL/min for 180 s after which the dissociation and the regeneration steps were performed as described above. For each set of experiments, a control run with protein only was performed to confirm that the chip surface was undergoing complete regeneration and validate that the results obtained among the experiments are comparable.

Apparent binding constants for the defined structures with sizes from dp8 to dp16 were evaluated based on an SPR solution affinity assay as previously described [32]. For each K_d measurement, samples containing 5 nM of $VEGF_{165}$ or 100 nM $VEGF_{55}$ with various concentrations of oligosaccharide (diluted from 1–10 mM stock solutions) were prepared in HBS-EP buffer. Binding was monitored using equivalent conditions for sample injection, dissociation, and regeneration conditions as described above. The process of protein (P) pre-equilibrated with ligand (L) can be expressed as:

$$P+L \rightleftharpoons P \cdot L \tag{1}$$

The equilibrium equation is:

$$[L][P]=K_d[L \cdot P] \tag{2}$$

The free concentrations at equilibrium for protein and ligand are:

$$[P]=[P]_{total}-[L \cdot P] \text{ and } [L]=[L]_{total}-[L \cdot P] \tag{3}$$

Substitution of these expressions into the equilibrium equation and rearranging and solving for $[L \cdot P]$ give:

$$[L \cdot P] = \frac{([L]_{\text{total}} + [P]_{\text{total}} + K_{\text{d}})}{2} - \sqrt{\frac{([L]_{\text{total}} + [P]_{\text{total}} + K_{\text{d}})^2}{4} - [L]_{\text{total}}[P]_{\text{total}}} \quad (4)$$

Therefore, free protein concentration can be expressed as:

$$[P] = [P]_{\text{total}} - \frac{([L]_{\text{total}} + [P]_{\text{total}} + K_{\text{d}})}{2} + \sqrt{\frac{([L]_{\text{total}} + [P]_{\text{total}} + K_{\text{d}})^2}{4} - [L]_{\text{total}}[P]_{\text{total}}} \quad (5)$$

If binding is not mass transport limited in which case the initial binding rate (r) is proportional to the concentration of free protein and the maximum binding rate (r_{m}) measured in the absence of ligand is proportional to the total protein concentration, free protein concentration can be calculated by:

$$[P] = \frac{r}{r_{\text{m}}}[P]_{\text{total}} \quad (6)$$

The initial binding response for each sensorgram was measured 10 s before the end of injection and was subsequently employed to estimate free protein concentration using equation 6. Calculated free protein concentration [P] was plotted against total oligosaccharide concentration $[L]_{\text{total}}$ and fit to equation 5 to determine apparent K_{d} values [32]. Analysis of duplicate or triplicate experiments was conducted at each oligosaccharide concentration in order to better estimate errors in the acquired data and fitted values.

RESULTS

Preparation of heparin-derived oligosaccharide library

As part of an ongoing effort in our laboratory to understand the highly complex structure of heparin and its structure-function relationships, a small structurally characterised heparin oligosaccharide library was assembled through the controlled, partial depolymerisation of porcine intestinal mucosa heparin using heparinase 1 and purification of the resulting cleavage products. This small library contains oligosaccharides of sizes between hexasaccharide (dp6) to hexadecasaccharide (dp16), with a number of these oligosaccharides being isolated and studied for the first time, affording new reagents for these heparin-binding protein activity studies.

Oligosaccharides with size ranging from dp6 to dp18 were examined in our study. Purified oligosaccharides from dp8 to dp16 in our library shared a common motif that made them particularly valuable for this structure-dependent binding study. These oligosaccharide motifs could be divided into three groups (**a**, **b** and **c**) differing in the five sugar residues located at their reducing end (Fig. 1). The components in each size group are structural analogs differing in the number of central trisulphated GlcNS6S-IdoA2S disaccharide units. The **a** motif consisted of only octasaccharide **8a** and decasaccharide **10a** since the distribution of this specific motif is susceptible to heparinase 1. The unique feature of the **a** motif is the presence of a glucuronic acid residue immediately adjacent to the reducing end. The **b** motif is characterised by cluster of trisulphated disaccharide repeating units of iduronic acid and glucosamine residues and is representative of canonical heparin structure. The **c** motif contains a four-residue stretch at its reducing end with a unique combination of sugar residue modifications that corresponds to a key portion of the high-affinity ATIII binding site in heparin (Fig. 1).

Binding kinetics of VEGF to immobilised heparin

SPR response curves were recorded for VEGF samples at a range of concentrations being injected and flowed over a heparin sensor chip. The binding kinetics and relative apparent affinities were calculated from these data as described in Methods and Materials and are summarised in Fig. 2 and Table 1. The sensorgrams of $VEGF_{165}$-heparin and $VEGF_{55}$-heparin binding displayed uniquely different shapes. Both sets of sensorgrams of $VEGF_{55}$-heparin and $VEGF_{165}$-heparin interaction fit well with the 1:1 Langmuir binding model consistent with a monophasic-binding process. The apparent microscopic on-rate and off-rate constants for $VEGF_{55}$-heparin binding were both greater than those for $VEGF_{165}$-heparin binding. Standard curves were constructed by plotting relative response values as a function of protein concentration (Fig. 2C and 2D). For both $VEGF_{165}$ and $VEGF_{55}$, the relative response from binding was detected to have a linear dependence on protein concentration with extrapolated fits that pass through the origin within experimental error, indicating that the binding experiments were not limited by mass transport.

Inhibition of VEGF association to heparin-coated chips by heparin-derived oligosaccharides

In the solution competition experiments, heparin oligosaccharides were pre-equilibrated with VEGF and the mixtures were passed over an immobilised heparin surface. Protein in complex with oligosaccharide in solution is distinguished from unbound protein in that the oligosaccharide bound state is not able to associate with heparin immobilised chip surface. The partitioning of VEGF in bound and unbound states results in a decrease in the binding response as compared to the control experiment obtained in the absence of oligosaccharide. Thus, productive binding of the oligosaccharides corresponds to a decrease in response that is directly related to the binding affinity for the formation of the VEGF-oligosaccharide complex. Uniform-sized oligosaccharide mixtures purified from fractionated heparin were first screened for their binding with $VEGF_{165}$ and $VEGF_{55}$. In Fig 3B, the relative VEGF-heparin binding responses in the presence of oligosaccharide are plotted as a percentage of the response detected in the control experiment and compared among oligosaccharides increasing in length from dp6 to dp18. As shown in Fig. 3, competition for binding to the chip surface was detected for both $VEGF_{165}$ and $VEGF_{55}$ exclusively in the presence of oligosaccharides containing eight or greater sugar residues. Competition from dp10 resulted in a stronger inhibition of ~35% for both proteins. Level of inhibition increased correspondingly with the increase in oligosaccharide chain length. The dp18 mixture, the largest fragment employed in this study, elicited a greater than 80% decrease in $VEGF_{165}$ binding to the chip surface. No detectable binding inhibition was seen by oligosaccharides with chain length shorter than dp8 (Fig. 3, dp2 and dp4 data not shown), even at relatively high oligosaccharide concentrations (i.e., no effect on heparin-VEGF binding was detected in the presence of dp6 in excess of 50 μM, data not shown). These results indicate that binding for $VEGF_{165}$ requires a heparin sequence longer than hexasaccharide.

Oligosaccharides with defined structures were next investigated to better understand VEGF binding specificity. Oligosaccharides composed entirely of trisulphated disaccharide units (structures in group **b**) exhibited the highest level of competitive binding to both $VEGF_{165}$ and $VEGF_{55}$ (Fig. 4). Octasaccharide **8a** and decassacharide **10a**, with a glucuronic acid residue adjacent to the reducing end, showed approximately 15% and 5% lower inhibition compared with their counterparts in group **b** for $VEGF_{165}$ and $VEGF_{55,}$ respectively. Oligosaccharides in group **c** showed the lowest binding capacity among the three structure motifs. This motif contains part of the high-affinity ATIII recognition site including a 3-*O*-sulpho group on the reducing end glucosamine and lacks 2-*O*-sulpho groups at the two hexuronic acid residues and one *N*-sulpho group at the glucosamine residue closest to the reducing end (see Fig. 1). An increase in oligosaccharide chain length was able to partially

offset the unfavorable sulphation pattern of group **c** structures, reflected by more similar levels of inhibition observed for motif **b** and **c** oligosaccharides at dp12, dp14 and dp16. The results suggest that, for a given sized oligosaccharide, binding for VEGF is highly dependent on their specific structures with respect to the degree of sulphation and backbone flexibility associated with the presence of IdoA residues. It is noteworthy that the unique 3-*O*-sulphation within heparin did not remarkably promote binding such that the effect of under sulphations of neighbouring residues could be counterbalanced.

K_D measurement by solution affinity assay

Quantification of apparent binding affinity of the heparin-derived oligosaccharides for VEGF binding was performed by analysis of SPR-based solution affinity experiments. In these competition binding studies, inhibition of VEGF association with the heparin immobilised on the chip surface was measured at varying concentrations of oligosaccharides. Apparent K_D values were calculated through fitting the SPR data that demonstrate the dependence of the relative binding responses on oligosaccharide concentration. A simplified binding model was employed to obtain the apparent K_D for both forms of VEGF in that no better fits were observed with more advanced models for $VEGF_{165}$ that contains two identical HS binding sites [33]. Representative SPR sensorgrams for $VEGF_{165}$-decasaccharide **10b** and $VEGF_{55}$-decasaccharide **10c** interactions are shown in Fig. 5A and 5B, respectively. For oligosaccharides with eight residues and greater, binding responses decreased with increasing oligosaccharide concentrations. Fig. 5C and 5D show plots of unbound VEGF as a function of total oligosaccharide from which the K_D was calculated. Apparent K_D values for each heparin-derived oligosaccharide are summarised in Table 2. Similar disassociation constants were obtained for $VEGF_{165}$ and $VEGF_{55}$ toward specific dp8 or dp10 oligosaccharides. As oligosaccharide length increased from dp10 to dp16, the apparent binding affinity increased from the low micromolar to the low nanomolar range. The apparent K_D values for the tetradecasaccharide and hexadecasaccharide were as low as ~100 nM which was nearly equivalent to the K_D measured here for $VEGF_{165}$ binding (80 nM) with unfractionated heparin, suggesting comparable protein binding affinity between heparin and heparin oligosaccharide with a size of dp14 and above. In all cases, the relative affinities among the three oligosaccharide motifs tested here demonstrate a VEGF binding preference toward motif **b** which contains the canonical sulphation pattern and sugar geometry of heparin in contrast to the alternative structures in motif **a** and **c** which are also commonly found in heparin and heparin sulphate materials (Table 2).

DISCUSSION

Emerging evidence now supports the view that VEGF is as a key anti-angiogenic target for various types of human cancers [13,14]. The VEGF family of growth factors regulates tumour angiogenesis by interacting with its receptors (VEGFR) through several different mechanisms [34]. Heparin and heparan sulphate regulate VEGF signal activation through driving a cooperative binding mechanism between VEGF and the co-receptor of VEGFR2, neuropilin [35]. Structural features within HS that promote VEGF-HS binding have been previously investigated by using HS-derived or HS-like oligosaccharides with various lengths and sulphation patterns [22,23]. However, there is a dearth of information on the capability of heparin-derived oligosaccharides for VEGF binding and signal activation. Although HS represents a major component in the ECM and on most cell surfaces, the greater affinity of VEGF toward heparin-derived oligosaccharides suggests that these provide a better foundation for constructing potent inhibitors that block formation and activation of the VEGF signaling complex relative to HS-derived candidates.

To provide greater insight into the structural determinates of heparin-VEGF recognition, the relative binding affinities were determined here for both $VEGF_{165}$ and $VEGF_{55}$ toward a

small structurally defined oligosaccharide library varying in length, sulphation patterns, and sugar ring geometries. Binding studies with this library provided for the systematic heparin binding characterization of $VEGF_{165}$ with regard to the size requirement for productive binding and preferred heparin-like structural aspects that are associated with greater sulphation and structural plasticity within heparin relative to HS.

Our data show that, for heparin-derived oligosaccharides, binding for both $VEGF_{165}$ and its heparin-binding domain $VEGF_{55}$ requires an oligosaccharide-binding partner that contains eight or more sugar residues. Purified heparin octasaccharide was found to inhibit VEGF binding to unfractionated heparin to a greater extent than an octasaccharide preparation containing a mixture of sulphation states and glucuronic acid compositions (Fig. 3 and 4). This result demonstrates that binding is dependent on the specific structure of an oligosaccharide. VEGF bound with strongest affinity toward octasaccharide **8b** consisting of repeating units of trisulphated IdoA-GlcN disaccharide and at a lesser degree toward undersulphated octasaccharides **8a** and **8c** (Fig. 4A and 4B). Smaller heparin oligosaccharides, including disaccharides, tetrasaccharide and hexasaccharide were unable to inhibit VEGF-heparin interaction, even at 50-fold higher concentration than required for binding of octasaccharide **8b** (data not shown). Previous reports on the solution structure of $VEGF_{55}$ suggested a minimum of heparin-derived hexasaccharide for binding and more recent molecular modeling studies revealed that a heparin hexasaccharide or heptasaccharide would be sufficient to occupy the heparin-binding cleft of $VEGF_{165}$ [23,24]. Our study has provided direct experimental evidence on the size requirement for VEGF-heparin binding using the single heparin binding fragment, $VEGF_{55}$. The observation that $VEGF_{55}$ failed to bind a heparin hexasaccharide in our study might be explained by a distinct minimum size requirement for VEGF binding under physiological conditions. In fact, for heparan sulphate oligosaccharides, dp10 was found to be the shortest size capable of binding $VEGF_{165}$ in physiological saline buffer [23]. In the current study we show, under the same physiological conditions, a heparin-derived octasaccharide consisting of mostly trisulphated disaccharide repeating units is the smallest oligosaccharide that can bind both $VEGF_{55}$ and $VEGF_{165}$. The one disaccharide unit difference in length between the minimum binding size of $VEGF_{165}$ for heparin and HS may come from a higher sulphation level of the heparin sequence. *In vivo* study has shown that heparin octasaccharides appear to inhibit VEGF-induced angiogenesis in H460 human lung carcinoma [36]. Nevertheless, longer oligosaccharides may be required for stronger inhibition against $VEGF_{165}$ and the $VEGF_{165}$-induced endothelial cell responses [22,37–38].

Our results also demonstrate that the minimum size of heparin oligosaccharide that conveys the equivalent apparent binding affinity with unfractionated heparin for $VEGF_{165}$ binding is a heparin tetradecasaccharides (dp14). Moreover, no significant difference was found for the binding constants of dp14 (90–100 nM) and dp16 (100–110 nM) with that of heparin measured in our experiment (80 nM) (Table 2), suggesting comparable $VEGF_{165}$ binding capability between these oligosaccharides and heparin. This finding provides an important guideline for the optimal size requirement in oligosaccharide based anti-tumour drug design. Previous studies found that heparin fragment of 16 or 18 sugar units inhibited the binding of $VEGF_{165}$ to its receptors while larger fragments potentiated the binding [39,40]. A number of LMWHs have been developed as potential anti-angiogenesis agents. Not surprisingly, the oligosaccharides comprising these polydisperse LMWH formulations contain species sufficiently long for supporting angiogenic cytokine activity including VEGF [41]. The occurrence of one of the common heparin-associated toxicity for oligosaccharide-based drugs, heparin-induced thrombocytopaenia (HIT), also depends on longer heparin oligosaccharides required for the formation of the antigenic complex with platelet factor 4 (PF4)[42]. Therefore, our data indicates that heparin oligosaccharides of the optimal lengths might be sufficient for $VEGF_{165}$ binding and inhibition and that longer compounds might

simply induce coagulation and autoimmune related side-effects without providing improved anti-angiogenic activity.

The oligosaccharide library we prepared represents the three prominent structure motifs within the heparin polysaccharide (Fig. 1). In our study we also investigated the VEGF binding affinity in response to each of these heparin structures. Experiments using defined oligosaccharide structures showed that the canonical trisulphated oligosaccharide (**b**) exhibited highest binding affinity for VEGF in each size class. This observation is consistent with previous findings on that 2-*O*, 6-*O* and *N*-sulpho groups in HS all contribute to the strength of protein binding [23]. The different binding capacity between oligosaccharide motif **a** and **b** indicate an important role of the iduronic acid residue for VEGF binding as previously reported, since the presence of 2-*O*-sulpho groups affect binding to a much lesser extent than *N*-sulpho and 6-*O* sulpho groups [43,44]. An undersulphated domain corresponding to a fragment of the antithrombin III binding site (**c**) appears to further reduce interaction with VEGF, suggesting the important contribution of *N*-sulpho group and that the addition of a 3-*O*-sulpho group can not compensate for the loss of the *N*-sulpho group.

We also characterised and compared the heparin binding properties between the full-length $VEGF_{165}$ and the single heparin binding fragment $VEGF_{55}$ to determine whether oligosaccharide binding is significantly influenced by structural regions beyond the heparin binding domain within $VEGF_{165}$. The SPR sensorgram for $VEGF_{55}$-heparin binding shows a different shape with that for $VEGF_{165}$-heparin binding suggesting differences in the binding kinetics. The ability of heparin oligosaccharides to inhibit VEGF binding to unfractionated heparin showed similar trend between $VEGF_{165}$ and $VEGF_{55}$. While nearly equivalent results were obtained for $VEGF_{55}$ and $VEGF_{165}$ with a particular octasaccharide, increasingly greater inhibition was observed for $VEGF_{165}$ by large oligosaccharides (dp>10). This observation was confirmed by the lower apparent K_D values for $VEGF_{165}$ binding with these larger oligosaccharides relative to $VEGF_{55}$. This apparent increase in affinity is likely due to the avidity effect of the $VEGF_{165}$ dimer in a cooperative binding mechanism provided by the linear array of polyvalent binding sites presented by extended heparin oligosaccharides [45]. It has also been previously reported that larger heparin fragments are able to simultaneously bind the two heparin binding domains of $VEGF_{165}$ and that such a bridging effect may stabilise and enhance binding [23,39]. However, modeling results suggest that oligosaccharides greater than 25 residues in length would likely be required for binding both heparin binding domains [23]. Interestingly, while the non-canonical heparin-like structure of motif **c** was tolerated within the binding site as demonstrated by appreciable binding affinity of the **8c**, the similar binding affinities between **12c** and **10b** and that between **14c** and **12b** suggest that little added benefit in binding affinity is provided when this motif is presented in addition to alternative binding units that contain canonical heparin structure. Our data from the binding studies with $VEGF_{55}$ clearly indicate that there is no significant difference between the intrinsic binding characteristics of the isolated heparin binding domain and the $VEGF_{165}$ dimer toward short oligosaccharides. These results offer novel insight into the binding properties of VEGF-heparin recognition that are free of the many inherent complications in interrogating the $VEGF_{165}$ dimer.

In conclusion, a heparin-derived oligosaccharide library with size ranging from dp6 to dp18 allowed us to better characterise the heparin-specific binding of $VEGF_{165}$. The minimum size among these heparin oligosaccharides for $VEGF_{165}$ binding under physiological conditions was an octasaccharide but a tetradecasaccharide bound $VEGF_{165}$ with comparable affinity to that of heparin. The trisulphated heparin oligosaccharides bound $VEGF_{165}$ with the greatest affinity. The relatively rapid rate constants and modest inherent affinity for $VEGF_{55}$-heparin association are consistent with a binding model where the heparin binding domain is able to rapidly sample alternative binding modes along heparin

chains in search of preferred Similar oligosaccharide libraries have been demonstrated to be useful in a number of previous studies for identification of critical structural features required for specific interactions with various HS binding proteins [46–53]. The SPR-based solution inhibition provides a fast and sensitive way for qualitative and quantitative screening of these libraries for candidates with maximum inhibitory effect towards protein-HS binding. Increasingly recognised for their therapeutic advantages due to a lower toxicity and a general effect towards multiple HS/heparin-dependent growth factors and metastasis related enzyme such as heparanases [54], heparin- and HS-derived oligosaccharides represent an exciting new approach for future anti-tumour drug development upon the elucidation of their structure-function relationship with the targeted angiogenic molecules.

Acknowledgments

FUNDING

This work was supported by grants from the funded by the National Institutes of Health GM38060 (RJL)

Abbreviations used

HS	heparin sulphate
LMWH	low molecular weight heparin
VEGF	vascular endothelial growth factor
VEGFR	vascular endothelial growth factor receptor
SPR	surface plasmon resonance
GAG	glycosaminoglycan
GlcA	glucuronic acid
IdoA	iduronic acid
GlcNAc	*N*–acetylglucosamine
GlcNS	*N*-sulphoglucosamine
GlcNS6S	6-*O*-sulpho-*N*-sulphoglucosamine
GlcNAc6S	6-*O*-sulpho-*N*–acetylglucosamine
GlcNS3S	3-*O*-sulpho-*N*-sulphoglucosamine
GlcNS3S6S	3,6-*O*-sulpho-*N*-sulphoglucosamine
ATIII	antithrombin III
PGs	proteoglycans
ECM	extracellular matrix
HBD	heparin binding domain
FGF	fibroblast growth factor
FLT-1	FMS-like tyrosine kinase
KDR	Kinase insert domain receptor
SA	streptavidin
HEPES	4-(2-hydroxyethyl)-1-piperazineethanesulphonic acid
EDTA	ethylenediaminetetraacetic acid

dp	degree of polymerization
SAX	strong anion exchange
HPLC	high-performance liquid chromatography
LC	liquid chromatography
MS	mass spectrometry
NMR	nuclear magnetic resonance
FC	flow cell
K_d	dissociation constant
RU	resonance unit
HIT	heparin-induced thrombocytopaenia
PF4	platelet factor 4

References

1. Casu B, Lindahl U. Structure and biological interactions of heparin and heparan sulfate. Adv Carbohyd Chem Bi. 2001; 57:159–206.
2. Linhardt RJ. Heparin: Structure and activity. J Med Chem. 2002; 46:2551–2564. [PubMed: 12801218]
3. Esko JD, Selleck SB. Order out of chaos: Assembly of ligand binding sites in heparan sulfate. Annu Rev Biochem. 2002; 71:435–471. [PubMed: 12045103]
4. Capila I, Linhardt RJ. Heparin - Protein interactions. Angew Chem-Int Edit. 2002; 41:391–412.
5. Lambaerts K, Wilcox-Adelman SA, Zimmermann P. The signaling mechanisms of syndecan heparan sulfate proteoglycans. Curr Opin Cell Biol. 2009; 21:662–669. [PubMed: 19535238]
6. Rodgers KD, Antonio JDS, Jacenko O. Heparan Sulfate Proteoglycans: A GAGgle of Skeletal-Hematopoietic Regulators. Dev Dyn. 2008; 237:2622–2642. [PubMed: 18629873]
7. Xian XJ, Gopal S, Couchman JR. Syndecans as receptors and organizers of the extracellular matrix. Cell Tissue Res. 2010; 339:31–46. [PubMed: 19597846]
8. Linhardt RJ, Toida T. Role of glycosaminoglycans in cellular communication. Accounts Chem Res. 2004; 37:431–438.
9. Ori A, Wilkinson MC, Fernig DG. The heparanome and regulation of cell function: structures, functions and challenges. Front Biosci. 2008; 13:4309–4338. [PubMed: 18508513]
10. Turnbull JE. Heparan sulfate glycomics: towards systems biology strategies. Biochem Soc Trans. 2010; 38:1356–1360. [PubMed: 20863313]
11. Ferrara N. Vascular Endothelial Growth Factor. Arterioscler Thromb Vasc Biol. 2009; 29:789–791. [PubMed: 19164810]
12. Moreira IS, Fernandes PA, Ramos MJ. Vascular endothelial growth factor (VEGF) inhibition--a critical review. Anticancer Agents Med Chem. 2007; 7:223–245. [PubMed: 17348829]
13. Hicklin DJ, Ellis LM. Role of the vascular endothelial growth factor pathway in tumor growth and angiogenesis. J Clin Oncol. 2005; 23:1011–1027. [PubMed: 15585754]
14. Niu G, Chen XY. Vascular Endothelial Growth Factor as an Anti-Angiogenic Target for Cancer Therapy. Curr Drug Targets. 2010; 11:1000–1017. [PubMed: 20426765]
15. Keyt BA, Berleau LT, Nguyen HV, Chen H, Heinsohn H, Vandlen R, Ferrara N. The carboxyl-terminal domain (111–165) of vascular endothelial growth factor is critical for its mitogenic potency. J Biol Chem. 1996; 271:7788–7795. [PubMed: 8631822]
16. Robinson CJ, Stringer SE. The splice variants of vascular endothelial growth factor (VEGF) and their receptors. J Cell Sci. 2001; 114:853–865. [PubMed: 11181169]

17. Ferro V, Dredge K, Liu L, Hammond E, Bytheway I, Li C, Johnstone K, Karoli T, Davis K, Copeman E, Gautam A. PI-88 and novel heparan sulfate mimetics inhibit angiogenesis. Semin Thromb Hemost. 2007; 33:557–562. [PubMed: 17629854]

18. Folkman J, Langer R, Linhardt RJ, Haudenschild C, Taylor S. Angiogenesis inhibition and tumor-regression caused by heparin or heparin fragment in the presence of cortisone. Science. 1983; 221:719–725. [PubMed: 6192498]

19. Mousa SA, Feng X, Xie J, Du Y, Hua Y, He H, O'Connor L, Linhardt RJ. Synthetic oligosaccharide stimulates and stabilizes angiogenesis: Structure-function relationships and potential mechanisms. J Cardiovasc Pharmacol. 2006; 48:6–13. [PubMed: 16954815]

20. Norrby K. 2.5 kDa and 5.0 kDa heparin fragments specifically inhibit microvessel sprouting and network formation in VEGF(165)-mediated mammalian angiogenesis. Int J Exp Pathol. 2000; 81:191–198. [PubMed: 10971740]

21. Norrby K, Ostergaard P. Basic-fibroblast-growth-factor-mediated de novo angiogenesis is more effectively suppressed by low-molecular-weight than by high-molecular-weight heparin. Int J Microcirc-Clin Exp. 1996; 16:8–15. [PubMed: 8739219]

22. Cole CL, Hansen SU, Barath M, Rushton G, Gardiner JM, Avizienyte E, Jayson GC. Synthetic Heparan Sulfate Oligosaccharides Inhibit Endothelial Cell Functions Essential for Angiogenesis. PLoS One. 2010; 5(7)

23. Robinson CJ, Mulloy B, Gallagher JT, Stringer SE. VEGF(165)-binding sites within heparan sulfate encompass two highly sulfated domains and can be liberated by K5 lyase. J Biol Chem. 2006; 281:1731–1740. [PubMed: 16258170]

24. Fairbrother WJ, Champe MA, Christinger HW, Keyt BA, Starovasnik MA. Solution structure of the heparin-binding domain of vascular endothelial growth factor. Structure. 1998; 6:637–648. [PubMed: 9634701]

25. Stauffer ME, Skelton NJ, Fairbrother WJ. Refinement of the solution structure of the heparin-binding domain of vascular endothelial growth factor using residual dipolar couplings. Journal of Biomolecular Nmr. 2002; 23:57–61. [PubMed: 12061718]

26. Sasisekharan R, Bulmer M, Moremen KW, Cooney CL, Langer R. Cloning and expression of heparinase-I gene from flavobacterium-heparinum. Proc Natl Acad Sci U S A. 1993; 90:3660–3664. [PubMed: 8475114]

27. Xiao ZP, Zhao WJ, Yang B, Zhang ZQ, Guan HS, Linhardt RJ. Heparinase 1 selectivity for the 3,6-di-O-sulfo-2-deoxy-2-sulfamido-alpha-D-glucopyranose (1,4) 2-O-sulfo-alpha-L-idopyranosyluronic acid (GlcNS3S6S-IdoA2S) linkages. Glycobiology. 2011; 21:13–22. [PubMed: 20729345]

28. Yang B, Solakyildirim K, Chang YQ, Linhardt RJ. Hyphenated techniques for the analysis of heparin and heparan sulfate. Anal Bioanal Chem. 2011; 399:541–557. [PubMed: 20853165]

29. Xiao ZP, Tappen BR, Ly M, Zhao WJ, Canova LP, Guan HS, Linhardt RJ. Heparin Mapping Using Heparin Lyases and the Generation of a Novel Low Molecular Weight Heparin. J Med Chem. 2011; 54:603–610. [PubMed: 21166465]

30. Hernaiz M, Liu J, Rosenberg RD, Linhardt RJ. Enzymatic modification of heparan sulfate on a biochip promotes its interaction with antithrombin III. Biochem Biophys Res Commun. 2000; 276:292–297. [PubMed: 11006120]

31. Toida T, Yoshida H, Toyoda H, Koshishi I, Imanari T, Hileman RE, Fromm JR, Linhardt RJ. Structural differences and the presence of unsubstituted amino groups in heparan sulphates from different tissues and species. Biochem J. 1997; 322:499–506. [PubMed: 9065769]

32. Cochran S, Li CP, Ferro V. A surface plasmon resonance-based solution affinity assay for heparan sulfate-binding proteins. Glycoconjugate J. 2009; 26:577–587.

33. de Mol NJ. Affinity constants for small molecules from SPR competition experiments. Methods Mol Biol. 2010; 627:101–111. [PubMed: 20217616]

34. Stuttfeld E, Ballmer-Hofer K. Structure and Function of VEGF Receptors. IUBMB Life. 2009; 61:915–922. [PubMed: 19658168]

35. Grunewald FS, Prota AE, Giese A, Ballmer-Hofer K. Structure-function analysis of VEGF receptor activation and the role of coreceptors in angiogenic signaling. BBA-Proteins Proteomics. 2010; 1804:567–580.

36. Hasan J, Shnyder SD, Clamp AR, McGown AT, Bicknell R, Presta M, Bibby M, Double J, Craig S, Leeming D, Stevenson K, Gallagher JT, Jayson GC. Heparin octasaccharides inhibit angiogenesis in vivo. Clin Cancer Res. 2005; 11:8172–8179. [PubMed: 16299249]
37. Ashikari-Hada S, Habuchi H, Kariya Y, Itoh N, Reddi AH, Kimata K. Characterization of growth factor-binding structures in heparin/heparan sulfate using an octasaccharide library. J Biol Chem. 2004; 279:12346–12354. [PubMed: 14707131]
38. Khorana AA, Sahni A, Altland OD, Francis CW. Heparin inhibition of endothelial cell proliferation and organization is dependent on molecular weight. Arterioscler Thromb Vasc Biol. 2003; 23:2110–2115. [PubMed: 12920044]
39. Soker S, Goldstaub D, Svahn CM, Vlodavsky I, Levi BZ, Neufeld G. Variations in the size and sulfation of heparin modulate the effect of heparin on the binding of VEGF(165) to its receptors. Biochem Biophys Res Commun. 1994; 203:1339–1347. [PubMed: 7522446]
40. Fuh G, Garcia KC, de Vos AM. The interaction of neuropilin-1 with vascular endothelial growth factor and its receptor Flt-1. J Biol Chem. 2000; 275:26690–26695. [PubMed: 10842181]
41. Norrby K, Nordenhem A. Dalteparin, a low-molecular-weight heparin, promotes angiogenesis mediated by heparin-binding VEGF-A in vivo. Apmis. 2010; 118:949–957. [PubMed: 21091776]
42. Mikhailov D, Young HC, Linhardt RJ, Mayo KH. Heparin dodecasaccharide binding to platelet factor-4 and growth-related protein-alpha–Induction of a partially folded state and implications for heparin-induced thrombocytopenia. J Biol Chem. 1999; 274:25317–25329. [PubMed: 10464257]
43. Faham S, Hileman RE, Fromm JR, Linhardt RJ, Rees DC. Heparin structure and interactions with basic fibroblast growth factor. Science. 1996; 271:1116–1120. [PubMed: 8599088]
44. Ono K, Hattori H, Takeshita S, Kurita A, Ishihara M. Structural features in heparin that interact with VEGF(165) and modulate its biological activity. Glycobiology. 1999; 9:705–711. [PubMed: 10362840]
45. McGhee JD, Hippel PHV. Theoretical aspects of DNA-protein interactions - cooperative and non-cooperative binding of large ligands to aone-dimensional homogeneous lattice. J Mol Biol. 1974; 86:469–489. [PubMed: 4416620]
46. Jemth P, Kreuger J, Kusche-Gullberg M, Sturiale L, Gimenez-Gallego G, Lindahl U. Biosynthetic oligosaccharide libraries for identification of protein-binding heparan sulfate motifs - Exploring the structural diversity by screening for fibroblast growth factor (FGF) 1 and FGF2 binding. J Biol Chem. 2002; 277:30567–30573. [PubMed: 12058038]
47. Barth H, Schafer C, Adah MI, Zhang FM, Linhardt RJ, Toyoda H, Kinoshita-Toyoda A, Toida T, van Kuppevelt TH, Depla E, von Weizsacker F, Blum HE, Baumert TF. Cellular binding of hepatitis C virus envelope glycoprotein E2 requires cell surface heparan sulfate. J Biol Chem. 2003; 278:41003–41012. [PubMed: 12867431]
48. Peterson FC, Elgin ES, Nelson TJ, Zhang FM, Hoeger TJ, Linhardt RJ, Volkman BF. Identification and characterization of a glycosaminoglycan recognition element of the C chemokine lymphotactin. J Biol Chem. 2004; 279:12598–12604. [PubMed: 14707146]
49. Zhang FM, Ronca F, Lindhardt RJ, Margolis RU. Structural determinants of heparan sulfate interactions with Slit proteins. Biochem Biophys Res Commun. 2004; 317:352–357. [PubMed: 15063764]
50. Suk JY, Zhang FM, Balch WE, Linhardt RJ, Kelly JW. Heparin accelerates gelsolin amyloidogenesis. Biochemistry. 2006; 45:2234–2242. [PubMed: 16475811]
51. Zhang FM, McLellan JS, Ayala AM, Leahy DJ, Linhardt RJ. Kinetic and structural studies on interactions between heparin or heparan sulfate and proteins of the hedgehog signaling pathway. Biochemistry. 2007; 46:3933–3941. [PubMed: 17348690]
52. Zhang FM, Zhang ZQ, Lin XF, Beenken A, Eliseenkova AV, Mohammadi M, Linhardt RJ. Compositional Analysis of Heparin/Heparan Sulfate Interacting with Fibroblast Growth Factor. Fibroblast Growth Factor Receptor Complexes. Biochemistry. 2009; 48:8379–8386. [PubMed: 19591432]
53. Ra HJ, Harju-Baker S, Zhang FM, Linhardt RJ, Wilson CL, Parks WC. Control of Promatrilysin (MMP7) Activation and Substrate-specific Activity by Sulfated Glycosaminoglycans. J Biol Chem. 2009; 284:27924–27932. [PubMed: 19654318]

54. Ilan N, Elkin M, Vlodavsky I. Regulation, function and clinical significance of heparanase in cancer metastasis and angiogenesis. Int J Biochem Cell Biol. 2006; 38:2018–2039. [PubMed: 16901744]

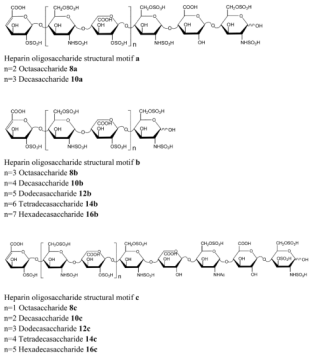

Figure 1.

Structures of heparin-derived oligosaccharides prepared using heparinase 1. Oligosaccharide sizes ranged from dp8 to dp16. Three prominent oligosaccharide motifs, labeled as **a**, **b** and **c**, were observed in members of this small library.

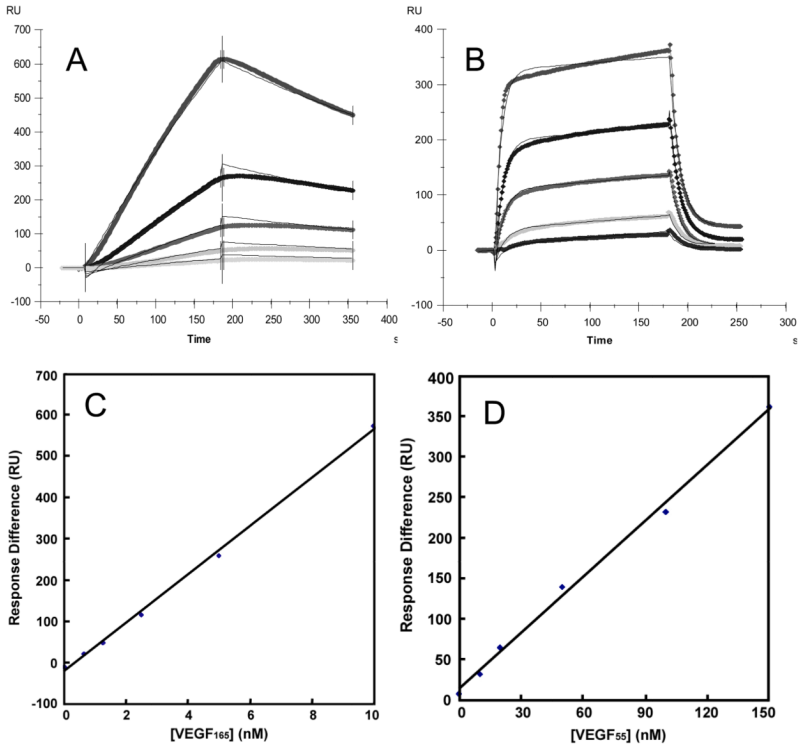

Figure 2.

Kinetics of $VEGF_{165}$- or $VEGF_{55}$-heparin interactions. SPR sensorgrams showing change in binding response to varying concentrations of injected proteins of (A) $VEGF_{165}$ from 0.63 to 10 nM (from bottom to top) and (B) $VEGF_{55}$ from 10 to 150 nM (from bottom to top). The thin black curves in (A, and B) are the fitting curves using models from BIA evaluate 4.0.1. Protein standard curve for (C) $VEGF_{165}$ and (D) $VEGF_{55}$ were prepared by plotting binding response (RU) as a function of injected protein concentration.

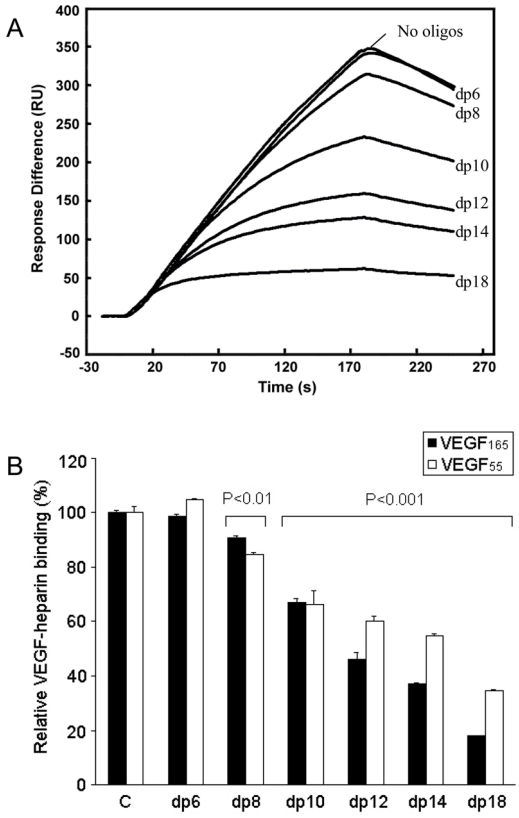

Figure 3.

Sized heparin oligosaccharide mixtures inhibit VEGF binding to heparin. (A) SPR sensorgrams demonstrating the change in binding response upon injection of 5 nM $VEGF_{165}$ pre-mixed without added oligosaccharide (upper curve) and with 1 μM sized mixture of heparin oligosaccharides from dp6 to dp18 in HBS-EP buffer flowed over a heparin chip. (B) Inhibitory effect of sized oligosaccharides on $VEGF_{165}$-heparin and $VEGF_{55}$-heparin binding. Binding response of VEGF with no added oligosaccharide is used as a control (c). Relative VEGF-heparin binding response from oligosaccharide treatment is expressed as a percentage of control. The bars are shown as mean values ± SD (n≥3).

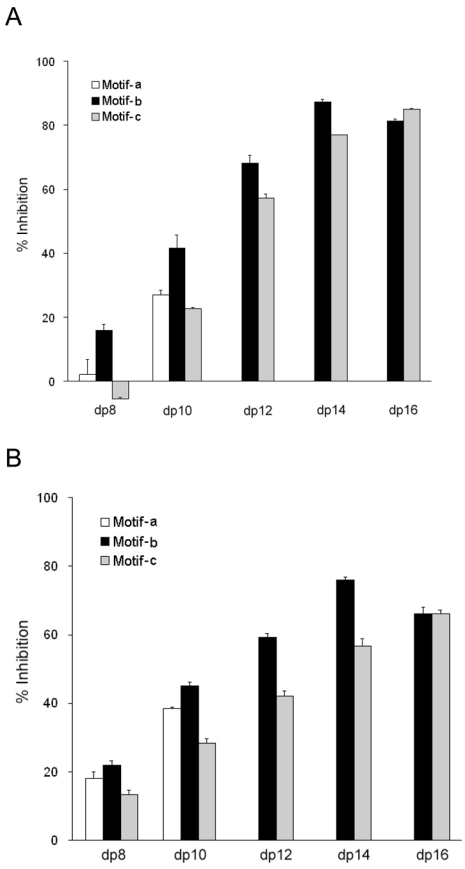

Figure 4.

Structurally-defined heparin oligosaccharides inhibit VEGF binding to heparin. 1 μM of each defined heparin oligosaccharide was pre-mixed with (A) 5 nM of $VEGF_{165}$ or (B) 100 nM of $VEGF_{55}$ in HBS-EP buffer and the mixture was passed over an immobilised heparin surface. Binding response from VEGF with no added oligosaccharide is used as a control. Decrease in binding response is expressed as an inhibition percentage of control. The bars are shown as mean values ± SD (n≥3).

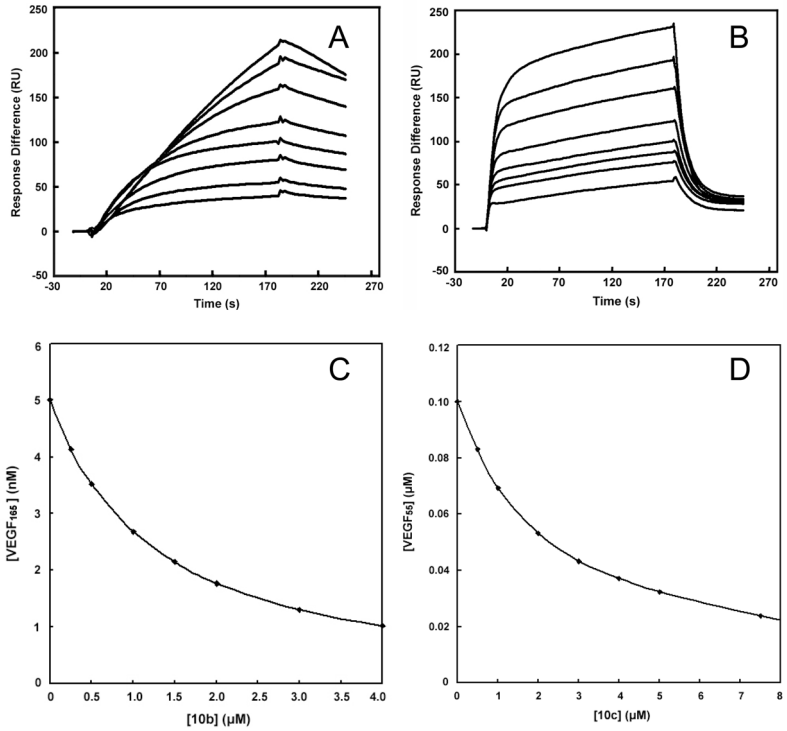

Figure 5.

Representative apparent K_D measurement for heparin decasaccharide binding to VEGF. SPR sensorgrams showing change in (A) 5 nM $VEGF_{165}$ binding to heparin upon treatment with varying concentrations of decasaccharide **10b** from 0 to 4 μM or (B) 100 nM $VEGF_{55}$ binding to heparin upon treatment with varying concentrations of decasaccharide **10c** from 0 to 8 μM. Free protein concentration was calculated and plotted as a function of total oligosaccharide concentration for (C) $VEGF_{165}$ and (D) $VEGF_{55}$. K_D was determined by fitting the data points in equation 1. See Methods section for details.

Table 1

Kinetics and relative apparent affinities of VEGF binding to immobilised heparin.

Interaction	k_{on}^{app} (1/MS)	k_{off}^{app} (1/S)	K_D^{app} (nM)	K_D (nM)[a]
$VEGF_{165}$ - heparin	8.6×10^3	6.9×10^{-4}	80	40 – 157
$VEGF_{55}$ - heparin	3.1×10^5	6.1×10^{-2}	197	N.R.

[a] Literature values

N.R. Not reported

Table 2

Summary of apparent K_D values for heparin-derived oligosaccharides binding with VEGF. Data shown in mean ± SD (n≥3).

Ligand		$VEGF_{165}$	$VEGF_{55}$
Hp dp8	**8a**	7.2 ± 0.4 μM	6.5 ± 0.8 μM
	8b	5.5 ± 0.7 μM	4.8 ± 0.4 μM
	8c	14.1 ± 3.3 μM	7.3 ± 1.0 μM
Hp dp10	**10a**	1.8 ± 0.4 μM	1.5 ± 0.1 μM
	10b	1.3 ± 0.3 μM	1.4 ± 0.2 μM
	10c	2.4 ± 0.3 μM	2.3 ± 0.1 μM
Hp dp12	**12b**	471 ± 96 nM	950 ± 200 nM
	12c	570 ± 38 nM	1.9 ± 0.2 μM
Hp dp14	**14b**	90 ± 5 nM	358 ± 49 nM
	14c	103 ± 11 nM	799 ± 191 nM
Hp dp16	**16b**	113 ± 26 nM	478 ± 54 nM
	16c	105 ± 14 nM	584 ± 105 nM